

ORIGINAL PAGE IS  
OF POOR QUALITY

## LIFE PREDICTION AND CONSTITUTIVE MODELS FOR ENGINE HOT SECTION

### ANISOTROPIC MATERIALS PROGRAM\*

G.A. Swanson, T.G. Meyer, and D.M. Nissley  
United Technologies Corp.  
Pratt & Whitney

### INTRODUCTION

The purpose of this program is to develop life prediction models for coated anisotropic materials used in gas turbine airfoils. In the program, two single crystal alloys and two coatings are being tested. These include PWA 1480, Alloy 185, overlay coating (PWA 286), and aluminide coating (PWA 273). Constitutive models are also being developed for these materials to predict the time independent (plastic) and time dependent (creep) strain histories of the materials in the lab tests and for actual design conditions. This nonlinear material behavior is particularly important for high temperature gas turbine applications and is basic to any life prediction system. This report will highlight some of the accomplishments of the program this year.

### SINGLE CRYSTAL CONSTITUTIVE MODEL

Two separate unified constitutive models for single crystal PWA 1480 have been formulated and are in the final stages of development. The first model, the "microscopic model", computes the inelastic quantities on the crystallographic slip systems. This model achieves the required directional properties as a consequence of resolving the summed slip system stresses and strains onto the global coordinate system. The second model, the "macroscopic model", uses global stresses and strains directly and employs anisotropic tensors operating on global inelastic quantities to achieve the required directional properties. The two models offer a trade between accuracy and physical significance and computing time requirements. The microscopic model is more accurate and is more physically significant in its formulation than the macroscopic model. However the macroscopic model is more computationally efficient, because integration of the evolutionary equations is required only for the six global stress/strain quantities rather than for each of the slip systems.

Cyclic stress/strain data at 871C (1600F) will be used to illustrate the behavior of the models. Figures 1 and 2 show test data from uniaxial bars oriented in three crystal directions:  $\langle 001 \rangle$ ,  $\langle 111 \rangle$ , and  $\langle 011 \rangle$ . These three orientations represent the extreme ends of the possible crystal orientations.

---

\* Work performed under NASA contract NAS3-23939.

The tests were conducted under controlled strain rates ranging from 0.001% per second to 1.0% per second.

The microscopic model models deformation on both the octahedral slip systems and the cube slip systems. The importance of including both slip systems can be shown by examining the results of inactivating the cube system terms. The model, thus modified, was fit to the  $\langle 001 \rangle$  data and subsequently used to predict the  $\langle 111 \rangle$  behavior. Figure 3 shows the correlation with the  $\langle 001 \rangle$  data is quite good, but the prediction for the  $\langle 111 \rangle$  data is poor. The good correlation with the  $\langle 001 \rangle$  data could have been expected since for a tensile bar in this orientation, only the octahedral slip systems have nonzero resolved shear stresses. The resolved shear stress on the cube slip systems is zero for this orientation. In contrast, a tensile bar oriented in the  $\langle 111 \rangle$  direction has nonzero shear stresses on both the octahedral and the cube slip systems. When cube slip terms are included in the model, the correlation with the  $\langle 111 \rangle$  and  $\langle 001 \rangle$  data is quite good as seen in Figure 4. The model constants in this case have been determined to best fit both the  $\langle 001 \rangle$  and the  $\langle 111 \rangle$  data. The accuracy of the full model is illustrated in Figure 5 by a prediction of data from a third orientation: the  $\langle 011 \rangle$  orientation. Comparison with the test data in Figure 2 shows the prediction is very good. The maximum difference seen between the micro model and test data for all three orientations, for stress ranges up to 2100 MPa (305 ksi) and over three orders of magnitude of strain rate is less than 62 MPa (9 ksi).

In the macroscopic model being developed, a single set of evolutionary equations are written using the global stresses and strains directly (i.e. not resolving them onto slip systems). The orientation dependence is achieved by including anisotropic tensors in the evolutionary equations for both inelastic strain and back stress. If the anisotropic tensor is included only in the equation for inelastic strain, the best correlation with  $\langle 001 \rangle$  and  $\langle 111 \rangle$  data resulted in a maximum stress error 2.5 times that achieved in the slip system based model. However, as shown in Figure 6, when the back stress components are allowed to evolve anisotropically, correlation of the  $\langle 001 \rangle$  and  $\langle 111 \rangle$  test data is comparable to that achieved with the slip system based model. The ability of the macroscopic model to predict other orientations is currently under investigation.

#### COATING CONSTITUTIVE MODEL

Five isotropic constitutive models were evaluated based on ability to correlate isothermal overlay coating behavior during stress relaxation and ability to predict thermomechanical behavior. The models evaluated were a classical formulation (e.g. Ref.1), Walker's isotropic formulation (Ref.2), a simplified form of Walker's isotropic formulation where back stress was assumed equal to zero, the Stowell model (Ref.3), and Moreno's Simplified Unified Approach (Ref.4).

Early evaluation of model correlation ability indicated little differences between the models. Additional isothermal cyclic stress relaxation tests were subsequently conducted to determine whether kinematic terms were necessary. To accomplish this, a 5 minute strain hold initiating at zero stress after unloading was incorporated into the test history. Experimental results from the test conducted at 649C (1200F) is presented in Figure 7. The positive relaxation observed during the 5 minute strain hold indicated that kinematic hardening was necessary to accurately represent the overlay coating response. As such, the 3 models which do not contain kinematic hardening formulations (i.e. classical, simplified Walker, and Stowell) were dropped from consideration.

Correlation of the isothermal stress relaxation information was best accomplished using the Walker model. The Moreno model as applied was generally unable to correlate the observed positive relaxation response largely as a result of the assumed back stress evolution equation:

$$\Delta\Omega = E_p \Delta\epsilon_{in} + \epsilon_{in}\Delta E_p$$

where:  $\Delta\Omega$  = back stress increment  
 $E_p$  = strain hardening slope in uniaxial tensile test  
 $\Delta\epsilon_{in}$  = inelastic strain  
 $\Delta\epsilon_{in}$  = inelastic strain increment  
 $\Delta E_p$  = change in  $E_p$  (with respect to temperature)

Moreno in his work on Hastelloy X (Ref.4) utilized a less rigorous back stress formulation which relied on a set of rules. This was considered cumbersome and, hence, the above formulation was adopted.

Prediction of an out-of-phase overlay coating hysteresis loop by the Walker and Moreno models is presented in Figure 8. Clearly, the Walker model is the more accurate, but the Simplified Unified Approach does predict the gross behavior and is also quite easy to apply, since only simple hand calculations are required.

Aluminide diffusion coating isothermal stress relaxation tests are in process. Because diffusion coatings depend largely on the substrate material, tests are conducted on 2 thicknesses of PWA 1480 material .13 and .25 mm (.005" and .010"). Initially, the overlay constitutive model (i.e. Walker) will be applied to both thicknesses and each material constant will then be plotted vs. PWA 1480 thickness and extrapolated to zero PWA 1480 thickness to obtain the "effective" coating material constants.

#### LIFE PREDICTION TESTS

Tests concentrated on gaining insight to coating/PWA 1480 substrate interactions during thermomechanical loading conditions. Critical fatigue experiments conducted on <001> and <111> PWA 1480 specimens with either overlay or aluminide coatings have shown that thermomechanical fatigue life is significantly influenced by the presence of a coating, coating structure (overlay or diffusion), substrate orientation, and strain-temperature-time path. Test results supporting these conclusions are presented in Figures 9 through 12. All lives are relative to specimen separation life, except in Figure 12 where coating cracking lives are also provided. Although not shown, coating cracking lives generally follow the same trends. Isothermal fatigue tests were primarily limited to overlay coated <001> PWA 1480 and were designed to provide initial life data for exercising life models. This particular coating/substrate orientation combination was chosen because it is the most understood from previous experience and material behavior standpoints.

The remainder of specimen coating/substrate orientation combinations are intended to obtain anisotropy and coating structure effects.

#### LIFE PREDICTION MODELS

Based on observed specimen cracking lives obtained from multiple acetate replications of each specimen, life must be separated into coating and substrate

components such as provided in the following equation:

$$N_{sep} = N_{ci} + N_{si} + N_{sp}$$

where:  $N_{ci}$  = Number of cycles to generate a crack through the coating.

$N_{si}$  = Additional cycles for coating crack to penetrate a small distance into the substrate. Initially defined as .13 mm (.005").

$N_{sp}$  = Additional cycles to grow crack to critical size.

$N_{sep}$  = Specimen separation life (50% stress range drop).

Initially, simple correlations of overlay coating cracking life ( $N_{ci}$ ) were considered: Coffin-Manson, Ostergren, actual tensile hysteresis energy, and another hysteretic energy approach based upon the concept of effective temperature (Ref.5). In the latter approach, effective temperature was assumed to be the midcycle temperature of the loading condition (i.e.  $(T_{min}+T_{max})/2$ ). These four correlations are presented in Figure 13. In each case, the overlay coating correlating parameters were determined by analysis using a one-dimensional 2-bar mechanism. The correlation lines shown in the figure represent a "hand-fit" curve passing through all the out-of-phase TMF test conditions and are intended to serve as a reference to qualitatively judge the correlations. Of the four, the tensile hysteretic energy model is best able to correlate the lives of the varied test conditions.

PWA 1480 substrate life modeling depends upon what is considered crack initiation vs. propagation. The methodology applied in this program initially defines substrate crack initiation as a crack which has penetrated .13 mm (.005") into the PWA 1480. Assuming a penny-shaped crack, this is consistent with a .15 to .25 mm (.006" to .010") surface crack. To verify the relationship between acetate replica observations and actual substrate cracking, substantial optical and Scanning Electron Microscopy (SEM) fractography has been conducted. Such investigations have indicated that overlay coating cracks do not penetrate into the PWA 1480 substrate during tests conducted at high temperature. Figure 14 is a schematic of the demarkation between temperatures where coating cracks do or do not penetrate into the PWA 1480.

TMF of a coated specimen (or component) is particularly complex because thermal growth mismatch between coating and substrate introduce biaxial stresses and strains during thermal cycling. Final model(s) will consider such biaxial conditions and more rigorous statistical evaluations of the model(s) will then be performed.

#### FUTURE

In the coming year, additional cyclic tests are planned to assist in life prediction model development. Also, in Option 1 of the program, life model development will be extended to airfoil root attachment temperatures, stress levels, and notch stress concentrations.

## ACKNOWLEDGEMENTS

The authors wish to recognize some of the individuals contributing to the progress of the program. Dr. Kevin P. Walker, of Engineering Scientific Software, Inc., originator and developer of the single crystal constitutive models and one of the coating constitutive models. At P&W, Messrs. Paul P. Norris, Indrik Linask, and many others are continuing to develop constitutive and life prediction models and overseeing and interpreting specimen tests; also, Messrs. Frank X. Ashland, Phillip D. Retzer, William A. Murphy, and Larry E. Durey for their support in specimen procurement and testing.

## REFERENCES

1. Kraus, H.: "Creep Analysis", John Wiley & Sons, Inc., New York, Chapter 2, 1980.
2. Walker, K. P.: "Research and Development Program for Nonlinear Structural Modeling with Advanced Time-Temperature Dependence Constitutive Relationships", NASA CR-165533, November, 1981.
3. Stowell, E. Z., et al: "Predicted Behavior of Rapidly Heated Metal in Compression", NASA TR R-59, 1960.
4. Moreno, V.: "Development of a Simplified Analytical Method for Representing Material Cyclic Response", NASA CR-168100, January, 1983.
5. Pejsa, P. N. and Cowles B. A.: "Thermal Mechanical Fatigue Life Prediction for Advanced Anisotropic Turbine Alloys", Journal of Engineering for Gas Turbine and Power, vol. 108, July, 1986. ASME no. 86-GT-124.

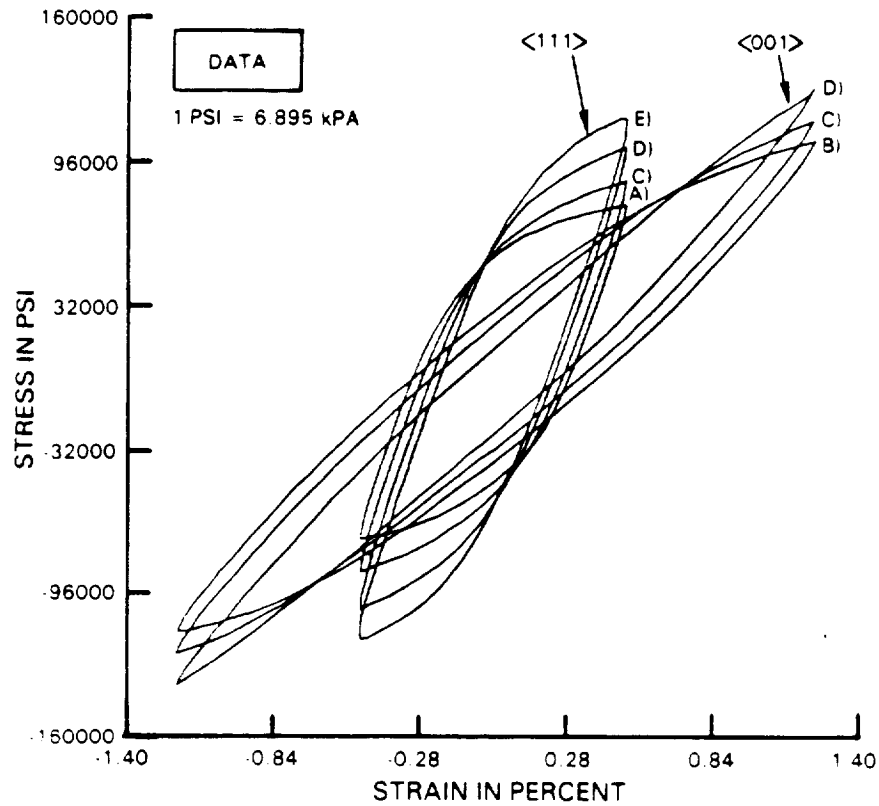


FIGURE 1 EXPERIMENTAL LOOPS IN  $\langle 001 \rangle$  AND  $\langle 111 \rangle$  DIRECTIONS AT 871C (1600F) AT STRAIN RATES OF A) .001% PER SEC, B) .0025% PER SEC, C) .01% PER SEC, D) .1% PER SEC, AND E) .5% PER SEC

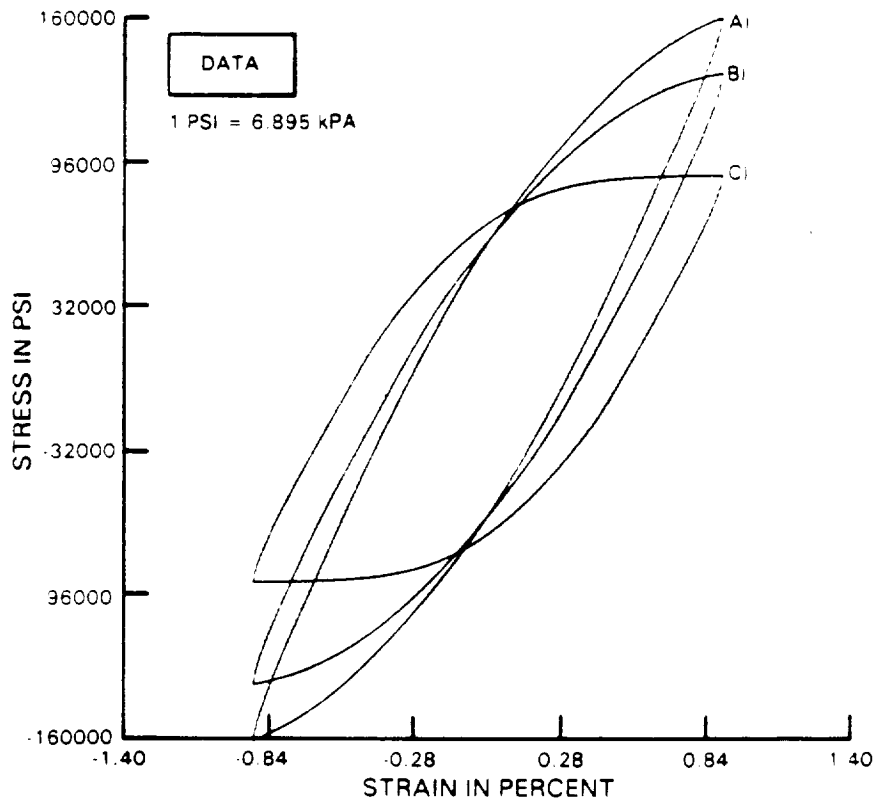


FIGURE 2 EXPERIMENTAL LOOPS IN  $\langle 011 \rangle$  ORIENTATION AT 871C (1600F) AT STRAIN RATES OF A) 1.0% PER SEC, B) 0.1% PER SEC, AND C) 0.001% PER SEC

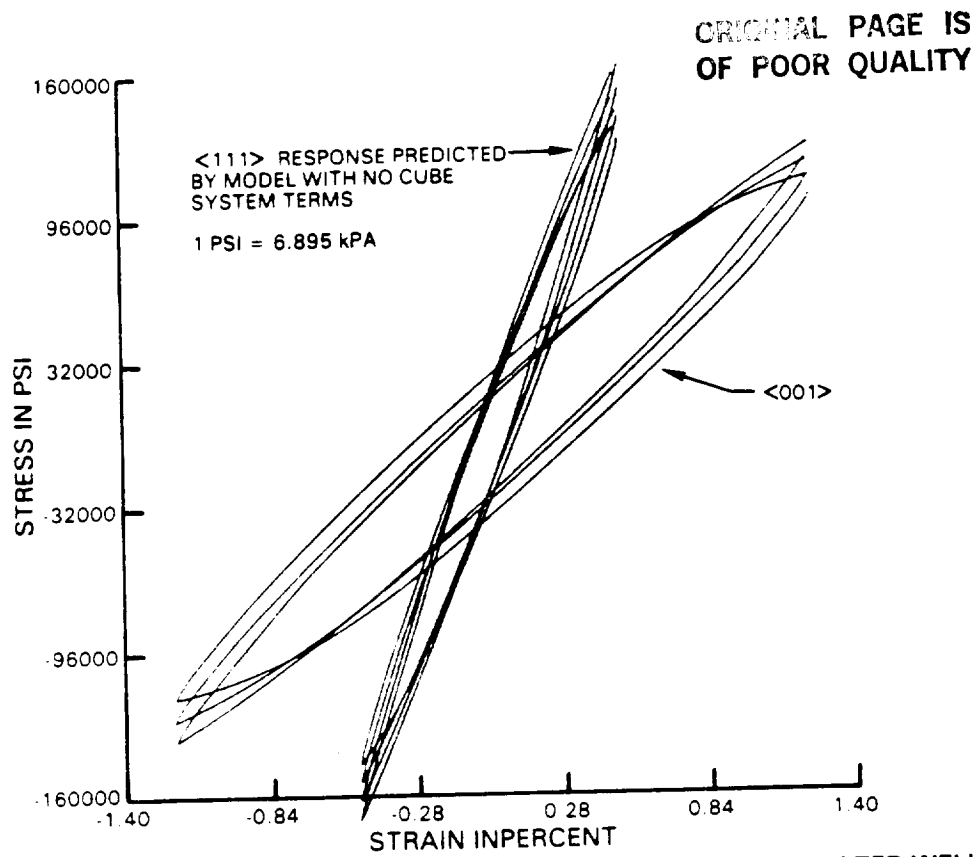


FIGURE 3 USING ONLY OCTAHEDRAL SLIP TERMS, THE  $\langle 001 \rangle$  DATA IS CORRELATED WELL BUT SUBSEQUENT PREDICTION OF  $\langle 111 \rangle$  RESPONSE IS POOR. COMPARE TO DATA IN FIGURE 1

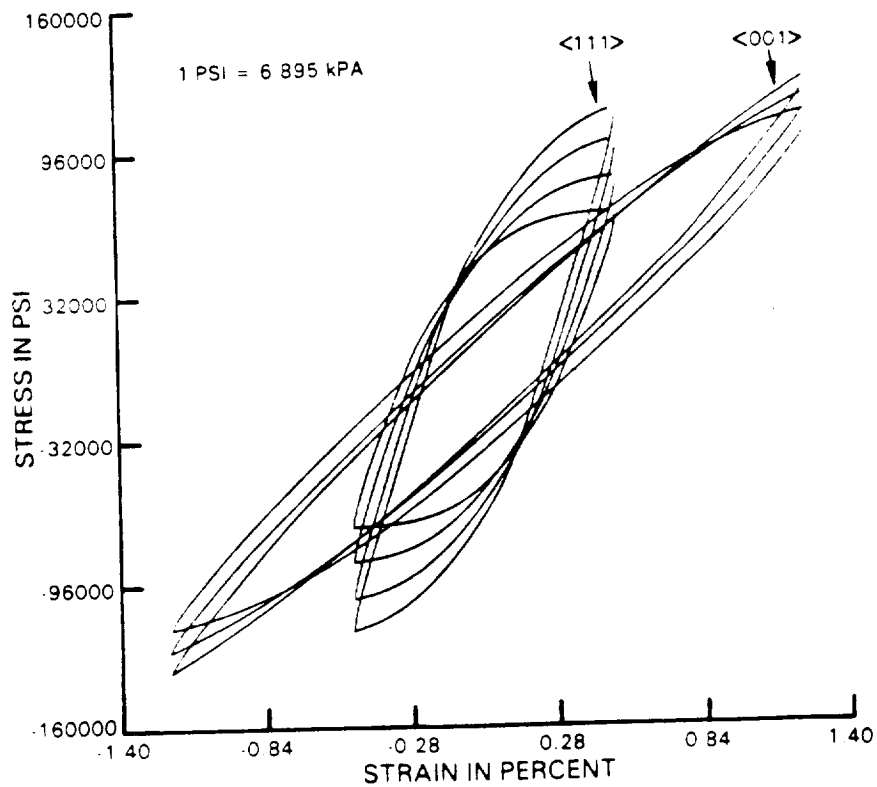


FIGURE 4 MICRO MODEL WITH BOTH OCTAHEDRAL AND CUBE SLIP TERMS CORRELATED TO  $\langle 111 \rangle$  AND  $\langle 001 \rangle$  DATA. COMPARE TO DATA IN FIGURE 1

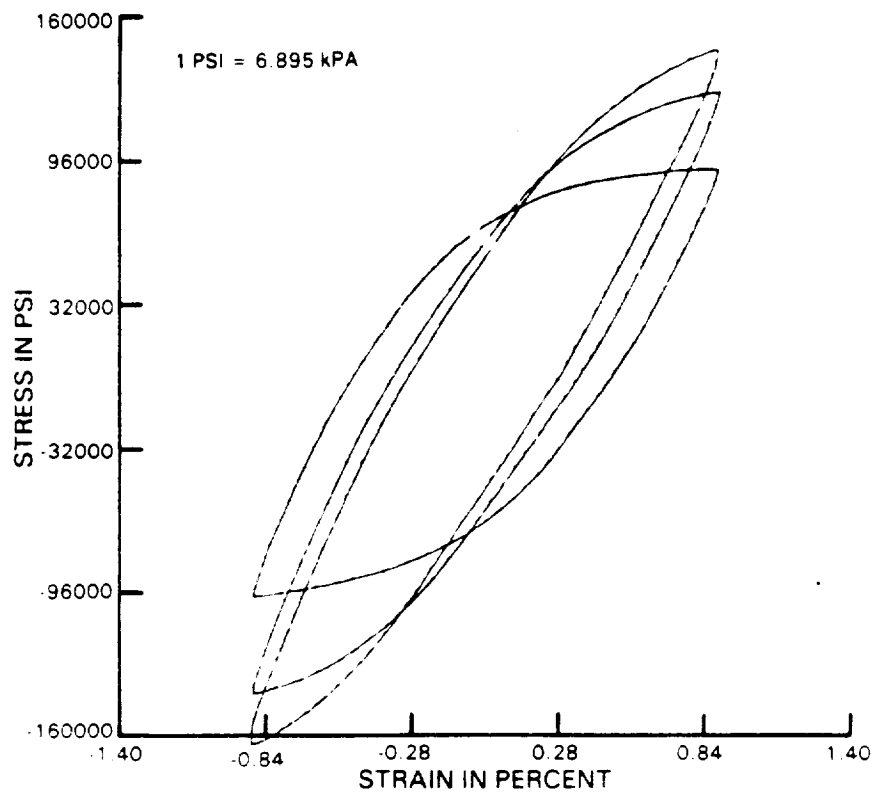


FIGURE 5 PREDICTED LOOPS IN  $\langle 011 \rangle$  ORIENTATION AT 871C (1600). COMPARE TO DATA IN FIGURE 2

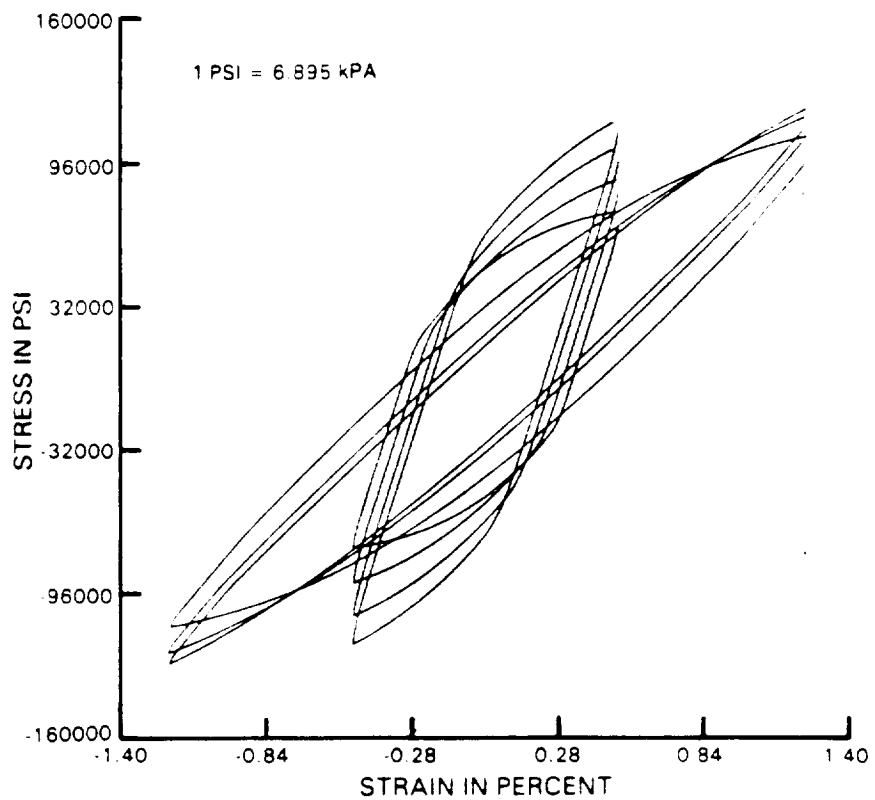


FIGURE 6 CORRELATION OF  $\langle 001 \rangle$  AND  $\langle 111 \rangle$  DATA WITH ANISOTROPIC BACK STRESS MODEL



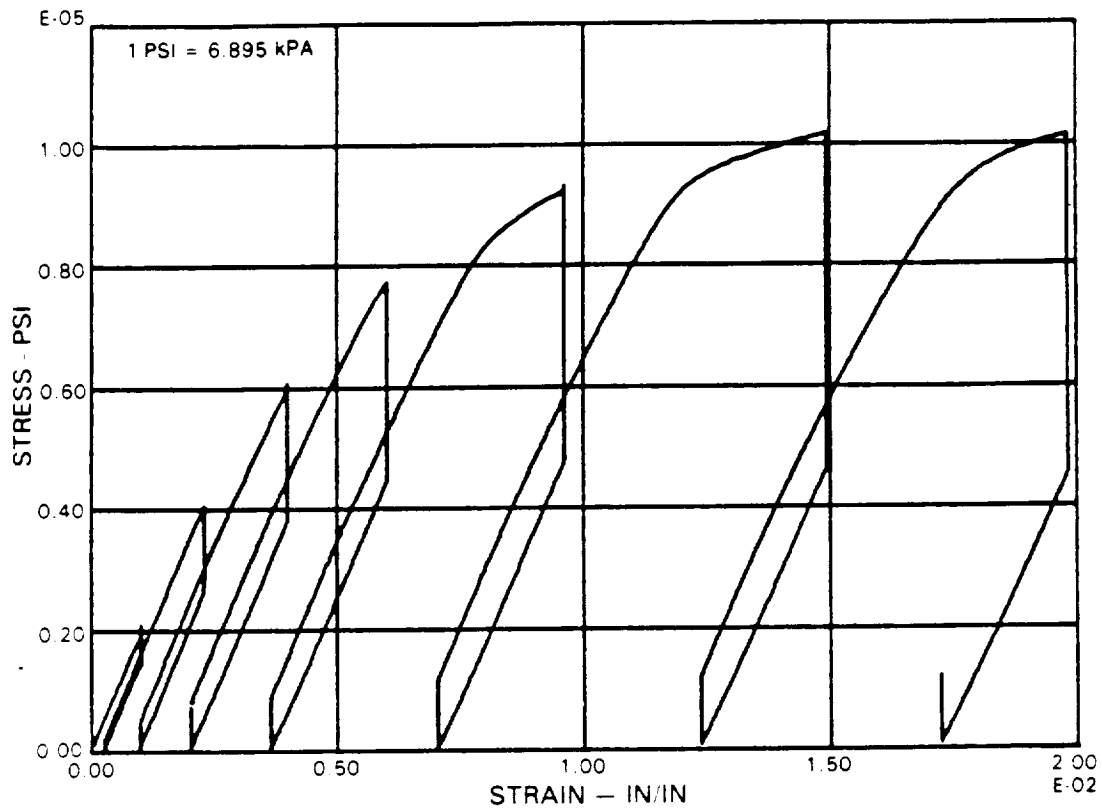


FIGURE 7 649°C (1200°F) STRESS RELAXATION TEST OF UNEXPOSED, BULK HIP'ED PWA286

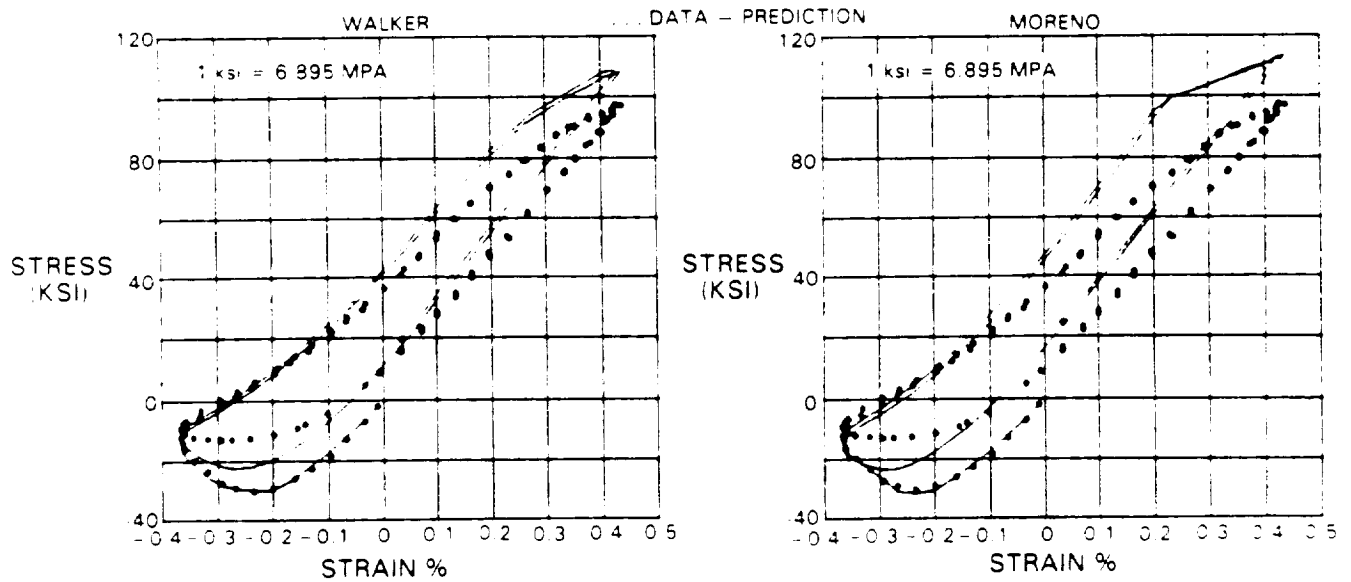
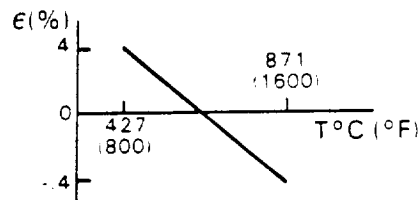
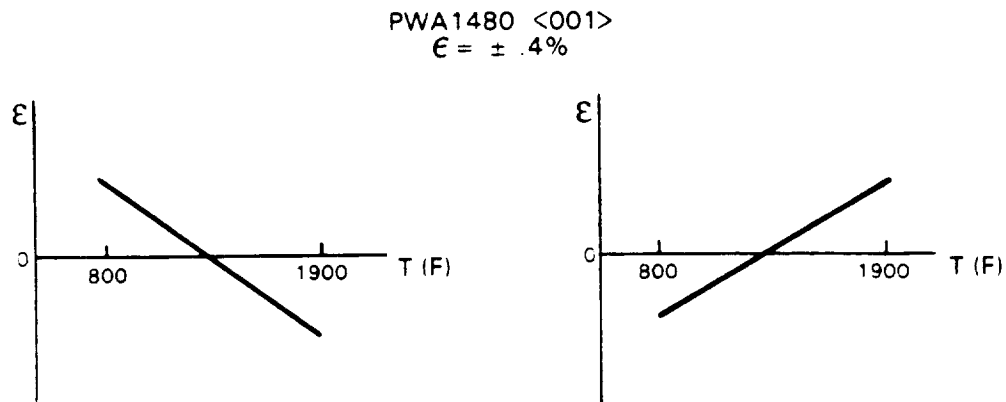


FIGURE 8 WALKER AND MORENO MODEL PREDICTION OF OUT-OF-PHASE TMF TEST



COATING		
NONE	1.00	2.35
PWA273 NiAl DIFFUSION	.22	4.00 -
PWA286 NiCoCrAlY OVERLAY	.73	4.06

FIGURE 9 THERMAL MECHANICAL FATIGUE LIFE DEPENDS UPON COATING

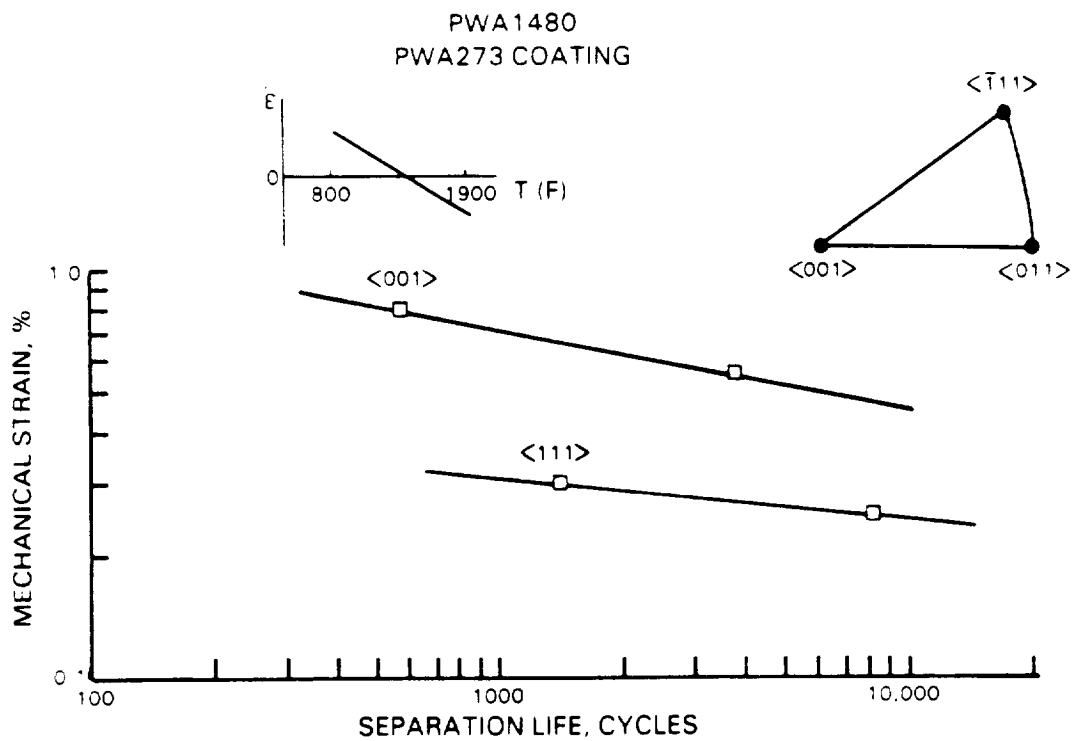


FIGURE 10 THERMAL MECHANICAL FATIGUE LIFE DEPENDS UPON SUBSTRATE ORIENTATION

ORIGINAL PAGE IS  
OF POOR QUALITY

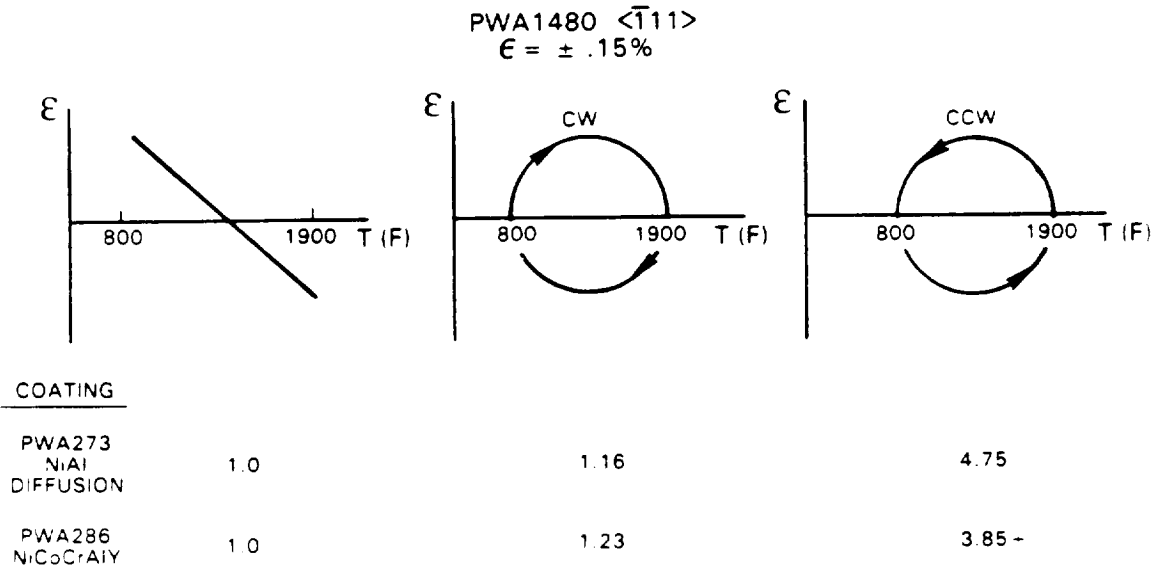


FIGURE 11 TMF LIFE DEPENDS UPON MECHANICAL STRAIN - TEMPERATURE PATH

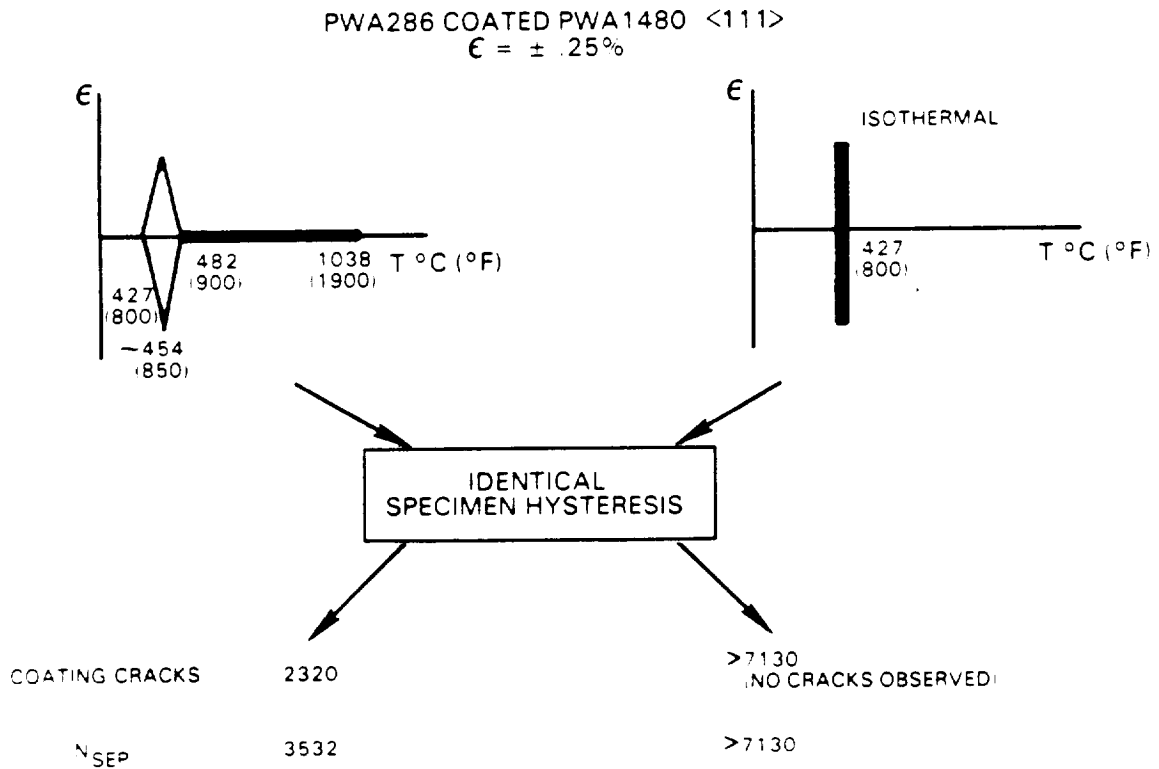


FIGURE 12 TMF LIFE DEPENDS UPON THERMAL CYCLE

ORIGINAL PAGE IS  
OF POOR QUALITY

+ 427C (800°F)  
\* 760C (1400°F)  
△ 927C (1700°F)  
X 1038C (1900°F)

● 421-1038C (800-1900°F) OUT-OF-PHASE TMF  
■ 427-1038C (800-1900°F) OTHER THAN OUT-OF-PHASE TMF  
○ 427-1149C (800-2100°F) OUT-OF-PHASE TMF

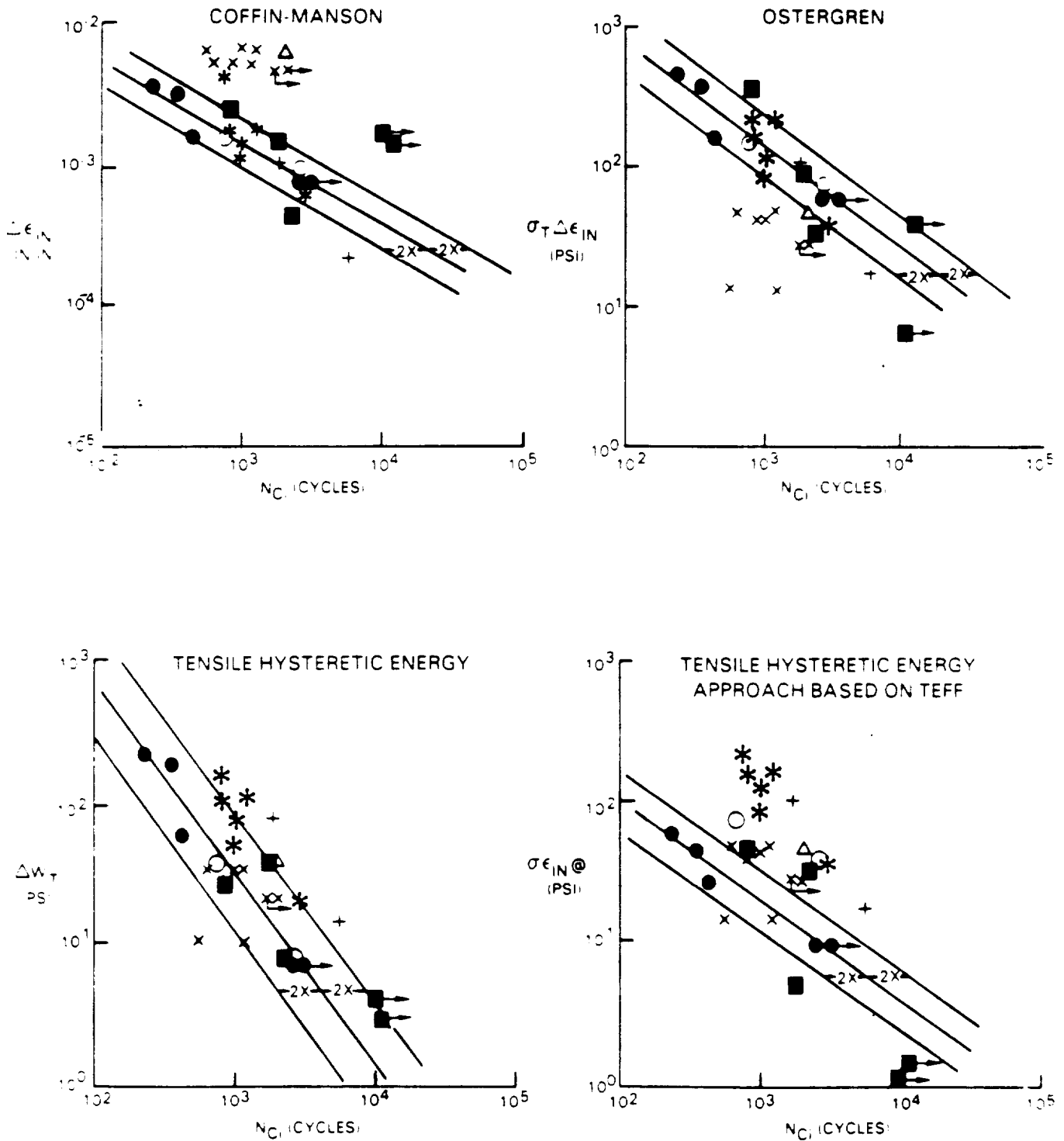


FIGURE 13 PWA286 OVERLAY COATING CRACKING LIFE CORRELATIONS

# PWA286 OVERLAY

# PWA273 ALUMINIDE

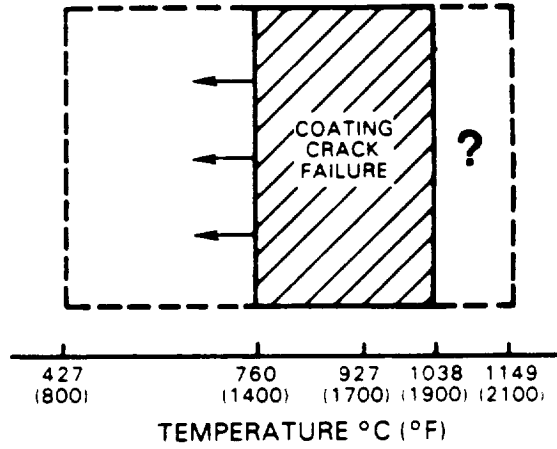
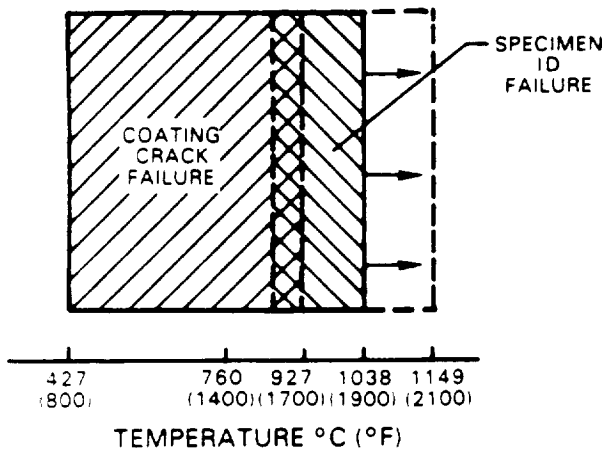


FIGURE 14 SCHEMATIC OF OBSERVED SPECIMEN FAILURES. AT HIGH TEMPERATURES PWA286 COATING CRACKS DO NOT PENETRATE INTO PWA1480.

—

1

2